Received: 20 April 2024 | Accepted: 26 July 2024

DOI: 10.1111/1462-2920.16689

BRIEF REPORT

ENVIRONMENTAL MICROBIOLOGY

Trophic strategies of picoeukaryotic phytoplankton vary over time and with depth in the North Pacific Subtropical Gyre

Kyle F. Edwards[1] | **Yoshimi M. Rii**[2] | **Qian Li**[3] | **Logan M. Peoples**[4] | **Matthew J. Church**[4] | **Grieg F. Steward**[5]

[1]Department of Oceanography, University of Hawai'i at Mānoa, Honolulu, Hawai'i, USA

[2]Hawai'i Institute of Marine Biology, University of Hawai'i at Mānoa, Kāne'ohe, Hawai'i, USA

[3]School of Oceanography, Shanghai Jiao Tong University, Shanghai Shi, China

[4]Flathead Lake Biological Station, University of Montana, Polson, Montana, USA

[5]Daniel K. Inouye Center for Microbial Oceanography: Research and Education, and Department of Oceanography, University of Hawai'i at Mānoa, Honolulu, Hawai'i, USA

Correspondence
Kyle F. Edwards, Department of Oceanography, University of Hawai'i at Mānoa, 1000 Pope Rd, Honolulu, 96822 Hawai'i, USA.
Email: kfe@hawaii.edu

Funding information
National Oceanic and Atmospheric Administration, Grant/Award Numbers: NA17RJ1223, NA090AR4320129; National Science Foundation, Grant/Award Number: 2224832; Simons Foundation, Grant/Award Number: 721221

Abstract

In oligotrophic oceans, the smallest eukaryotic phytoplankton are both significant primary producers and predators of abundant bacteria such as *Prochlorococcus*. However, the drivers and consequences of community dynamics among these diverse protists are not well understood. Here, we investigated how trophic strategies along the autotrophy-mixotrophy spectrum vary in importance over time and across depths at Station ALOHA in the North Pacific Subtropical Gyre. We combined picoeukaryote community composition from a 28-month time-series with traits of diverse phytoplankton isolates from the same location, to examine trophic strategies across 13 operational taxonomic units and 8 taxonomic classes. We found that autotrophs and slower-grazing mixotrophs tended to prevail deeper in the photic zone, while the most voracious mixotrophs were relatively abundant near the surface. Within the mixed layer, there was greater phagotrophy when conditions were most stratified and when Chl *a* concentrations were lowest, although the greatest temporal variation in trophic strategy occurred at intermediate depths (45–100 m). Dynamics at this site are consistent with previously described spatial patterns of trophic strategies. The success of relatively phagotrophic phytoplankton at shallower depths in the most stratified waters suggests that phagotrophy is a competitive strategy for acquiring nutrients when energy from light is plentiful.

INTRODUCTION

In the ocean, small eukaryotic phytoplankton often contribute a large fraction of primary production, especially in nutrient-poor environments (Pasulka et al., 2013; Rii et al., 2016). These unicellular protists come from a disparate array of evolutionary lineages (Choi et al., 2020; Pierella Karlusich et al., 2020), and most of these lineages include phago-mixotrophs that prey on other organisms in addition to performing photosynthesis (Li et al., 2022; Mitra et al., 2023). In oligotrophic waters, the cyanobacterium *Prochlorococcus* is a major component of the ecosystem (Partensky et al., 1999) and a potentially significant source of nutrition for phagotrophs. Previous work has shown that protistan predators of *Prochlorococcus* are taxonomically diverse (Frias-Lopez et al., 2009; Li et al., 2022; Wilken et al., 2023), and significant functional diversity has been documented among the mixotrophic taxa, with substantial variation in rates of ingestion across groups (Li et al., 2022). In addition, mixotrophic taxa with higher ingestion rates tend to have lower phototrophic performance and lower assimilation efficiency of prey biomass, leading to a spectrum of mixotrophic strategies (Edwards, Li, McBeain, et al., 2023; Li et al., 2022). Integrating these experimental trait measurements with *Tara* Oceans survey data (De Vargas et al., 2015) shows that phytoplankton trophic strategies shift across major environmental gradients: relatively phagotrophic taxa are more prevalent under stratified, low chlorophyll *a* (Chl *a*) conditions, and at shallower depths, while autotrophs and relatively

autotrophic mixotrophs are more prevalent under less stratified, high Chl *a* conditions, and deeper in the photic zone (Edwards, Li, McBeain, et al., 2023). These patterns are consistent with theoretical predictions that relatively phagotrophic phytoplankton are better competitors when dissolved nutrients are scarce and that they can better compete with heterotrophs when light is also plentiful (Edwards, 2019; Rothhaupt, 1996; Ward et al., 2011).

Outstanding questions include how the functional composition of smaller phytoplankton changes over time, and what environmental variables drive these changes. Studies have documented temporal dynamics in protistan plankton communities, as well as substantial community stratification across depths within the photic zone (e.g., Blanco-Bercial et al., 2022; Choi et al., 2020; Yeh & Fuhrman, 2022). A detailed survey of picoeukaryote dynamics over several years in the oligotrophic North Pacific found recurrent seasonal community changes, as well as shorter-term fluctuations driven by deep mixing events and mesoscale processes (Rii et al., 2022). Community dynamics depended on depth within the photic zone, with more consistent seasonal dynamics at shallower depths, and episodic variation deeper in the photic zone associated with temporary displacement of isopycnal depths (Rii et al., 2022). Understanding how these shifts in community composition translate into functional changes is important for understanding the causal mechanisms structuring communities, as well as the consequences for ecosystem and biogeochemical processes. For example, a shift from relatively autotrophic to relatively phagotrophic phytoplankton is expected to alter nutrient cycling and primary production (Mitra et al., 2014), as mixotrophs likely excrete less dissolved nutrients than heterotrophs, while using ingested prey nutrients to enhance total carbon fixation. Similarly, relatively phagotrophic phytoplankton may alter food web and export processes by transferring prey biomass more efficiently to higher trophic levels, relative to heterotrophic consumers (Edwards, Li, & Steward, 2023; Ward & Follows, 2016).

In this study, we synthesized a time-series of picoeukaryote relative abundances from the oligotrophic North Pacific (Rii et al., 2022) together with lab-measured data on the trophic strategies of diverse taxa isolated from the same location (Edwards, Li, McBeain, et al., 2023; Li et al., 2022). We asked whether the ability of phytoplankton taxa to ingest prey correlates with their environmental niches, including depth differences and temporal patterns at seasonal and shorter-term scales. We also explored how community-scale trophic strategy may shift with depth and time based on the subset of the community studied here. Finally, we considered whether the observed dynamics of trophic strategies at this site are consistent with environmental drivers previously identified in large-scale spatial comparisons (Edwards, Li, McBeain, et al., 2023).

EXPERIMENTAL PROCEDURES

Picoeukaryote metabarcoding time series

Methods for collection and analysis of the picoeukaryote time series are described fully in Rii et al. (2022). To summarize, samples were collected from eight depths (5, 25, 45, 75, 100, 125, 150, and 175 m) on 19 research cruises to Station ALOHA (22°45′ N, 158°00′ W) in the NPSG between February 2011 and May 2013. Two-litre seawater samples for DNA extraction were collected using a CTD rosette, prefiltered via peristaltic pump through 3 μm pore size polycarbonate membrane filters, and collected onto 0.2 μm pore size polyethersulphone filters. Filters were flash-frozen and stored at −80°C until DNA extraction. The V9 regions of 18S rRNA genes were amplified and sequenced via Illumina MiSeq pair-end sequencing (300 cycles). Sequences were trimmed and quality filtered, and reads were clustered into operational taxonomic units (OTUs) with UCLUST v1.2.22q, initially clustered with the SILVA 119 database and then clustered de novo at a 97% nucleotide identity threshold. Taxonomy was assigned to representative OTU sequences with BLAST (max E-value 10^{-30}), using the pre-clustered PR^2 database v.4.12.0 (Guillou et al., 2012). This yielded 29,062 distinct picoeukaryote OTUs with an average sequencing depth of ∼29,000 reads per sample. Raw sequence data was deposited into NCBI's Sequence Read Archive as BioProject ID PRJNA351881 (accession SRP092782). Contextual environmental data (photosynthetically active radiation, mixed layer depth, nutrient concentrations, picoeukaryote cell concentration, Chl *a* concentration, temperature, salinity, sea-level anomaly) were collected as described in Rii et al. (2022).

Phytoplankton isolates

Phytoplankton isolates and corresponding trait measurements used in this study were previously described (Edwards, Li, McBeain, et al., 2023; Li et al., 2022). To summarize, all strains were isolated from the euphotic zone at Station ALOHA and were maintained as unialgal but not axenic cultures at 24°C in 0.2 μm-filtered and autoclaved ALOHA seawater, under a 12:12 light:dark cycle with irradiance ∼70 μmol photons m^{-2} s^{-1}. Mixotrophs (as described in Li et al., 2022) were maintained in K medium without added nitrogen, amended with *Prochlorococcus* prey. Four isolates (*Ostreococcus*, *Chloropicon*, *Micromonas*, and *Pelagomonas*) did not grow when fed *Prochlorococcus* as the only added nitrogen source. These strains were maintained in full K medium and will be referred to as "autotrophs," while acknowledging they may take up organic compounds osmotrophically. Strain taxonomy

was characterized with phylogenetic analysis of 18S rRNA gene sequences as described in Li et al. (2022).

Grazing ability of mixotrophs was quantified as body volume-specific clearance rate when fed $\sim 10^6$ cells mL^{-1} *Prochlorococcus*. This trait was used because it has been measured on a large number of isolates (Li et al., 2022), and because it is negatively correlated with growth efficiency when consuming prey (Li et al., 2022) and negatively correlated with phototrophic growth rate (i.e., growth rate when provided dissolved nutrients and light but no added prey; Edwards, Li, McBeain, et al., 2023). As described previously, the clearance rates measured with these isolates approximate their maximum clearance rates, because prey concentrations were low enough to not saturate the ingestion rate (Li et al., 2022). Isolates determined to be autotrophic by mixotrophy assays were given a grazing ability of zero.

Matching isolates to OTUs

Isolates were matched to time-series OTUs by comparing near-full length 18S rRNA gene sequences of the isolates to all OTU reference sequences using nucleotide BLAST (Table S1). Some isolates are closely related (Li et al., 2022) and matched to the same OTU; the clearance rates of these isolates were averaged for the purpose of comparing grazing ability to OTU niches. In nearly all cases, the OTU with the lowest E-value (which quantifies the number of hits expected by chance) was frequent enough to analyse abundance patterns across the time-series samples (using a minimum occurrence threshold of 40 samples), and this OTU was chosen for further analysis. In some cases, there was a second OTU with an equivalent E-value but <10 reads, and this OTU was not used. In one case (the prasinophyte *Chloropicon*), three abundant OTUs had the same E-value, and their reads were summed in each sample for further analysis (choosing one OTU produced similar results). Strains of the dictyochophyte *Florenciella* formed two clades (Li et al., 2022), and strains from these two groups best matched two different *Florenciellales* OTUs. We matched an isolate of the bolidophyte *Triparma eleuthera* with the OTU annotated as *Triparma eleuthera*, because the best BLAST match of this isolate was the same OTU as an *Triparma mediterranea* isolate (and this OTU was annotated as *Triparma mediterranea*). In all cases, taxonomic annotation of the OTUs was consistent with isolate taxonomy independently derived by phylogenetic analysis of isolate 18S rRNA and related sequences from GenBank and the PR^2 database (Li et al., 2022). In total, the isolate matching process allowed us to match 21 isolates to 15 OTUs; after summing the three *Chloropicon* OTUs and averaging clearance rates of isolates matching to the same OTU, we obtained 13 distinct taxa (hereafter referred to as OTUs) whose niches could be compared to lab-measured grazing ability.

Statistical methods

Statistical methods were similar to those described in Edwards, Li, McBeain, et al. (2023). We asked whether the environmental niches of phytoplankton OTUs are correlated with their grazing ability. OTU niche axes were chosen a priori to test whether the trait-niche relationships previously found when analysing *Tara* Oceans metabarcoding samples are also present in the picoeukaryote community at Station ALOHA. The depth niche of OTUs was quantified as the slope of OTU relative abundance vs. depth in a generalized linear mixed model (GLMM). The relationship between OTUs and stratification was quantified as the slope of OTU relative abundance in mixed layer samples vs. mixed layer depth in a GLMM. To examine whether the recent history of stratification was more informative than contemporaneous stratification, we also used mean mixed layer depth over the prior 7 or 14 days, calculated from WHOTS subsurface sensor data as described in Rii et al. (2022), and defining mixed layer depth using a temperature difference of 0.2°C relative to temperature at 15 m (de Boyer Montégut et al., 2004). Finally, the relationship between OTUs and Chl *a* concentration was quantified as the slope of OTU relative abundance in mixed layer samples vs. mean mixed layer Chl *a* concentration.

OTU relative abundances were modelled using the beta-binomial distribution with a logit link function. For the depth analysis, the model had the form: $\text{logit}(p_{ij}) = \text{Isolate}_i + \text{Cruise}_j + \text{IsolateCruise}_{ij} + (\text{CR}_i * \text{CReff} + \text{slope}_i) * \text{Depth}_k$, $\text{reads}_{ij} \sim \text{BetaBinom}(p_{ik}, V_i, N_k)$. Here p_{ij} is the probability that a metabarcode read in sample j is from OTU i, Isolate_i is an OTU-specific random intercept capturing variation in mean relative abundance across OTUs, Cruise_j is a random effect capturing variation in mean relative abundance of all OTUs across cruises, $\text{IsolateCruise}_{ij}$ is a random effect capturing variation in mean relative abundance of OTU i across cruises, CR is specific clearance rate of OTU i, CReff is the effect of clearance rate on OTU responses to the environment, slope_i is a species-specific random slope capturing variation in depth niches not attributable to CR, Depth_k is the depth of sample k, reads_{ik} is number of reads of OTU i in sample k, V_i is an OTU-specific dispersion parameter, and N_k is the total number of phytoplankton reads in sample k. In summary, this model quantifies whether the relationship between relative abundance and depth for an OTU is predicted by that OTU's clearance rate. The GLMM approach is appropriate because it models the number of reads while accounting for variation in total reads, and allows for uncertainty in relative abundances and environmental relationships while quantifying CReff. For the analysis using mixed

layer depth, the model had the form logit(p_{ij}) = $Isolate_i$ + $Cruise_j$ + $IsolateCruise_{ij}$ + $Depth_m$ + $IsolateDepth_{im}$ + (CR_i*CReff + $slope_i$)*MLD_k, $reads_{ij}$ ~ BetaBinom(p_{ik}, V_i, N_k), where $Depth_m$ and $IsolateDepth_{im}$ are additional random effects to account for depth variation while analysing temporal changes in OTU relative abundance, and MLD_k is the mixed layer depth corresponding to sample *k*. The analysis of Chl *a* had the same model structure, but with log(Chl *a*) concentration in the place of MLD.

The assumption of logit-linear environmental responses in the GLMMs was largely appropriate based on visual inspection of the data (Figures 1, 3, and 4), although a few OTUs exhibited unimodal depth

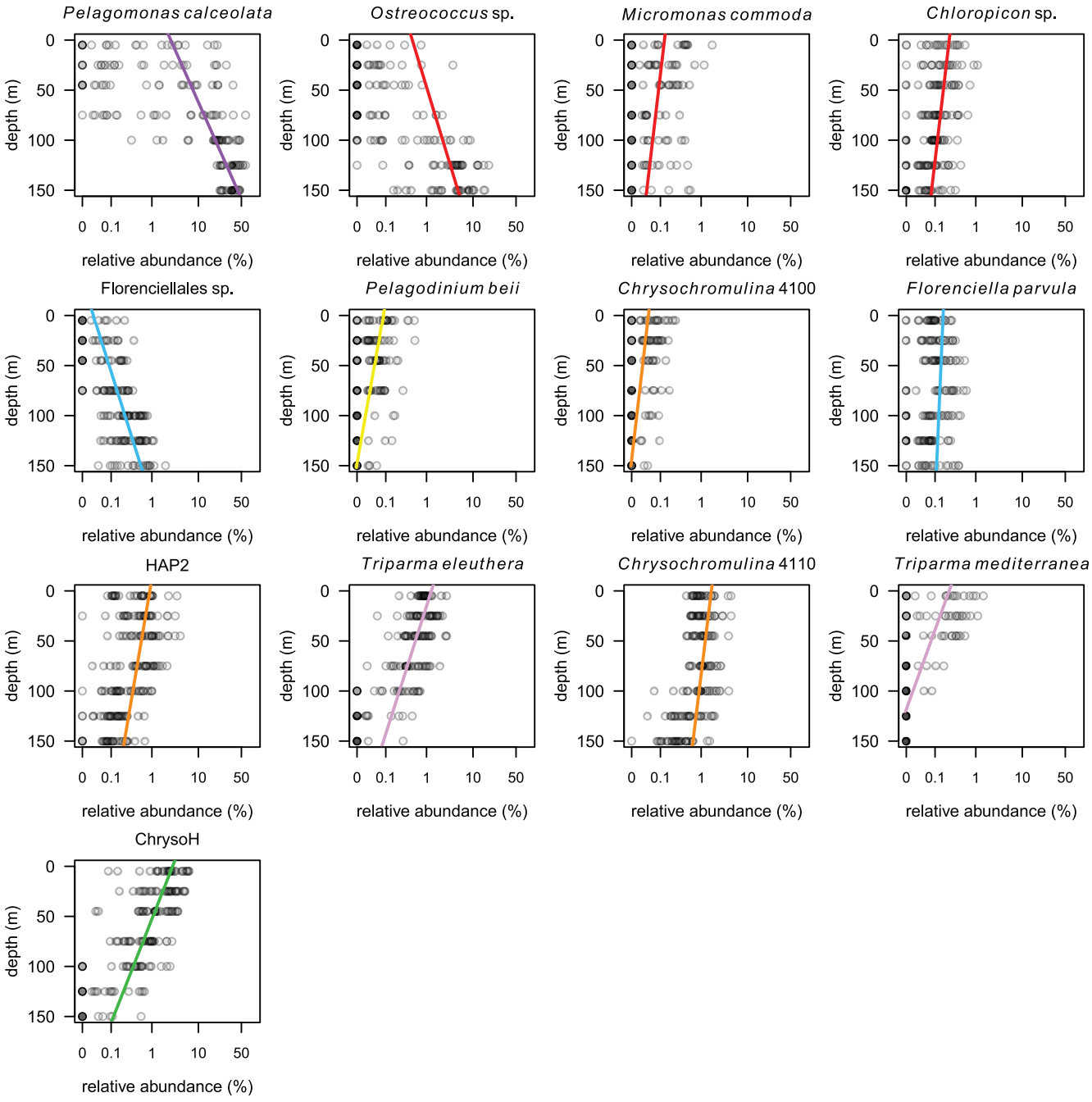

FIGURE 1 Depth niches of the phytoplankton OTUs analysed in this study. Relative abundance (proportion of reads) is plotted vs. depth, and the curves display the fitted logistic functions from a beta-binomial GLMM. The slope parameters of these curves are subsequently compared to the grazing ability of the corresponding isolate (Figure 2). To facilitate visual comparison of OTU slopes, the x-axes are logit transformed and have the same limits on each panel. Panels are titled using the name of the corresponding isolate. The four top panels are autotrophs, and the subsequent mixotroph panels are sorted by grazing ability from left to right and top to bottom. Colours of the fitted curves correspond to the taxa colour scheme in Figure 2 (purple = pelagophyte, red = prasinophyte, blue = dictyochophyte, yellow = dinoflagellate, orange = haptophyte, purple = bolidophyte, green = chrysophyte).

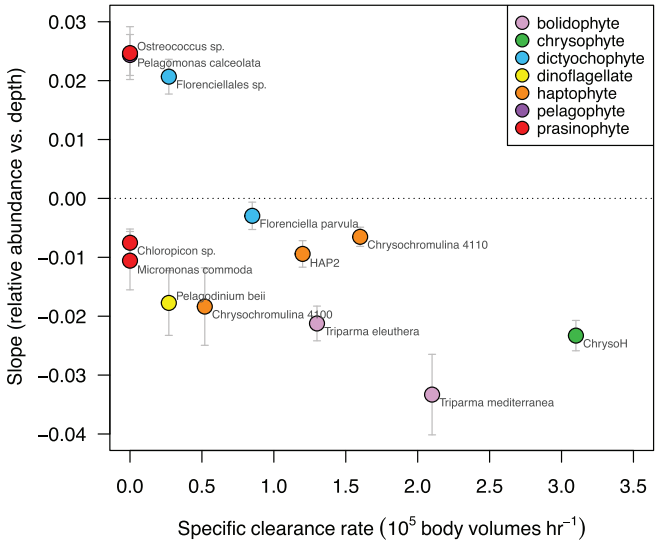

FIGURE 2 Depth niches of phytoplankton OTUs compared to their grazing abilities. The y-axis is the slope of relative abundance vs. depth from a beta-binomial GLMM (Figure 1), with 95% CI error bars. The x-axis is grazing ability quantified as the body volume-specific clearance rate when consuming *Prochlorococcus*. Four autotrophic OTUs are given values of zero on the x-axis. Text adjacent to the points displays the names of the isolates.

profiles (e.g., *Florenciella parvula* and HAP2; Figure 1). To consider nonlinear niche relationships in the same GLMM framework, we also fit models where the environmental variables were treated as categorical predictors, which allowed for flexible nonlinear relationships. The depth categories were the set of standard sampling depths, while MLD and Chl *a* were binned into 5 and 6 equal-sized bins, respectively. Models were fit in R using the package glmmTMB (Brooks et al., 2017). All niche analyses were performed with two datasets: the full set of 13 OTUs including autotrophs and mixotrophs, and the set of 9 mixotroph OTUs. This allowed us to test for drivers of diversity within the mixotrophs, and also test whether including autotrophs as endmembers of the trophic spectrum yields consistent results. To define the total number of phytoplankton reads, we summed the reads of known phytoplankton taxa (Bacillariophyta, Bolidophyceae, Chlorarachniophyceae, Chlorodendrophyceae, Chlorophyceae, Chloropicophyceae, Chrysophycea, Cryptophyceae, Dictyochophyceae, Euglenozoa, Mamiellophyceae, Pavlophyceae, Pelagophyceae, Phaeophyceae, Pinguiophyceae, Prymnesiophyceae, Pyramimonadales, Trebouxiophyceae, other haptophytes, other chlorophytes, other prasinophytes). Dinoflagellates, with the exception of the focal OTU *Pelagodinium*, were excluded from the total phytoplankton read counts because of the difficulty in assigning phototrophic vs. heterotrophic status to all taxa. However, using the total number of all picoeukaryote reads (i.e., including heterotrophic taxa and dinoflagellates) instead of the total number of phytoplankton reads yielded nearly identical results when testing relationships between grazing ability and OTU niches.

Community mean trait dynamics

To assess how seasonal and episodic dynamics of trophic strategies vary with depth, we calculated a community average trophic strategy. This average was defined as the weighted mean clearance rate of the focal phytoplankton community, where the weights are the relative abundances of the focal phytoplankton taxa. Because we do not have clearance rate data (or tests of mixotrophy for putative autotrophs) for all phytoplankton taxa, we make several assumptions to construct an average trait value, with the recognition that this analysis is a coarse approximation meant to capture broad trends in trophic strategy. We assume that the clearance rates measured on the isolates are representative of their genera, and we assign the mean clearance rate of a genus to all reads from that genus, using the genera assigned to our OTUs using the PR^2 database. For three OTUs from undescribed genera (Florenciellales_X, Haptophyta_Clade_HAP2_XXX, and Chrysophyceae_Clade-H_X), we sum the reads from these clades. The dinoflagellate *Pelagodinium* was omitted from this analysis, because its corresponding OTU was annotated at a very coarse level (Dinophyceae_XXX). Using the summed relative abundance of all taxa in each genus, and corresponding clearance rates (with zeros assigned to autotrophs), we calculated a weighted mean clearance rate of the focal phytoplankton community. We visually explore the dynamics of the mean trait over time, with the rationale that the diverse set of genera in this study are a reasonable proxy for the trophic strategy of the whole picoeukaryote phytoplankton community. On average, these genera account for 38% of total reads of the non-dinoflagellate phytoplankton taxa.

RESULTS

Trophic strategies across depths in the photic zone

As described previously (Rii et al., 2022), picoeukaryote taxa at Station ALOHA exhibit different depth niches within the photic zone (Figure 1). For example, *Pelagomonas* and *Ostreococcus* show a steep increase in relative abundance below ~75 m, while *Triparma* and chrysophyte clade H have the greatest relative abundance in the top 50 m. Previous analyses of phytoplankton trophic strategies in the global ocean found a shift from phototrophy to phagotrophy when moving from deeper to shallower depths in the photic

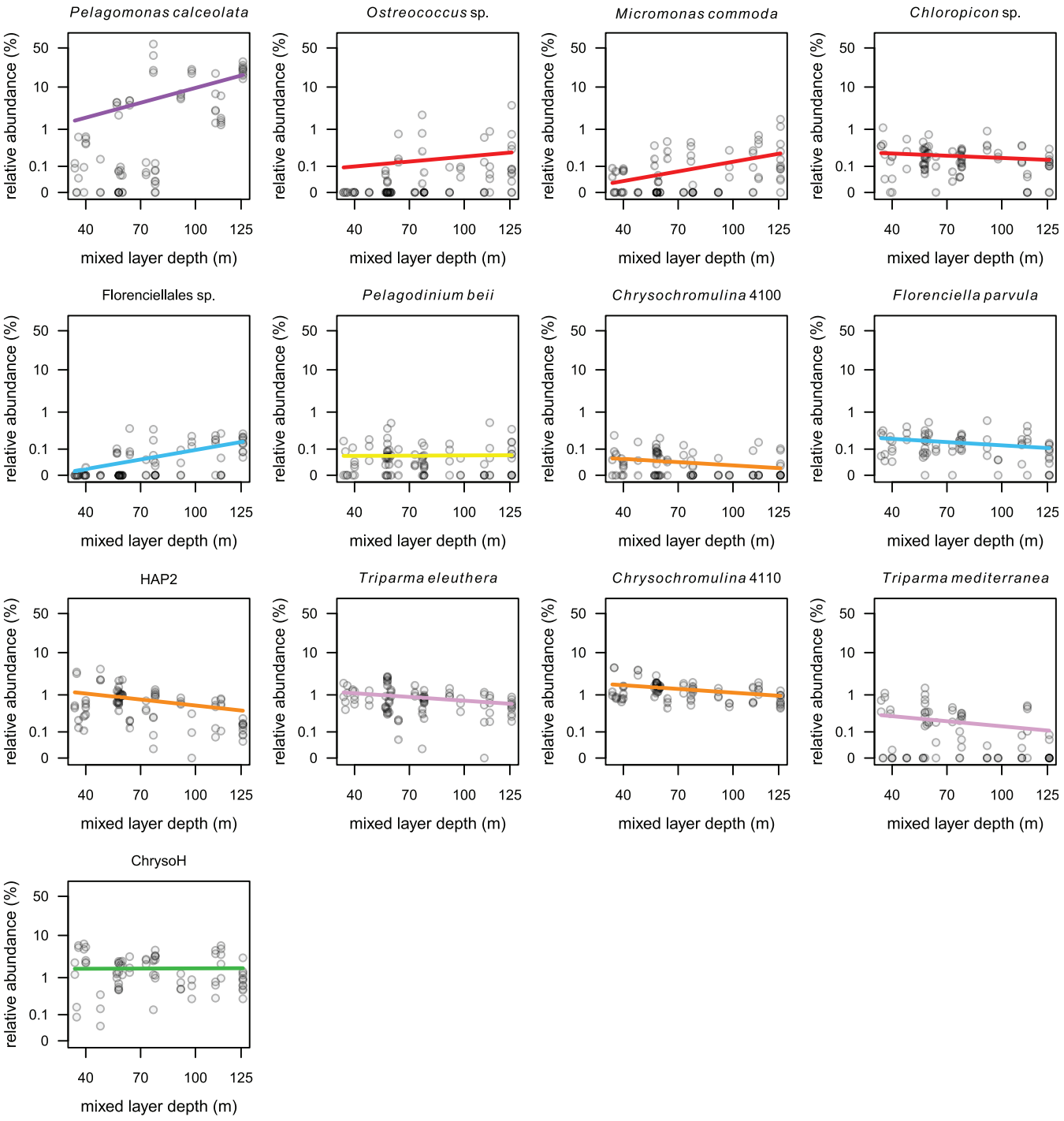

FIGURE 3 Niches of phytoplankton OTUs in response to variation in mixed layer depth. Relative abundance (proportion of reads) of samples within the mixed layer is plotted vs. mean mixed layer depth over the prior 14 days, and the curves display the fitted logistic curves from a beta-binomial GLMM. The slope parameters of these curves are subsequently compared to the grazing ability of the corresponding isolate (Figure 5A). To facilitate visual comparison of OTU slopes, the y-axes are logit transformed and have the same limits on each panel. Panels are titled using the name of the corresponding isolate. The four top panels are autotrophs, and the subsequent mixotroph panels are sorted by grazing ability from left to right and top to bottom. Colours of the fitted curves correspond to the taxa colour scheme in Figure 2 (purple = pelagophyte, red = prasinophyte, blue = dictyochophyte, yellow = dinoflagellate, orange = haptophyte, purple = bolidophyte, green = chrysophyte).

zone (Edwards, Li, McBeain, et al., 2023). In the current study, autotrophs are represented by OTUs and isolates of the pelagophyte genus *Pelagomonas* and the prasinophyte genera *Ostreococcus*, *Micromonas*, and *Chloropicon*. Mixotrophs are represented by the haptophyte genus *Chrysochromulina* (2 OTUs) and clade HAP2, the dictyochophyte genus *Florenciella* (2 OTUs), the bolidophyte genus *Triparma* (2 OTUs), the

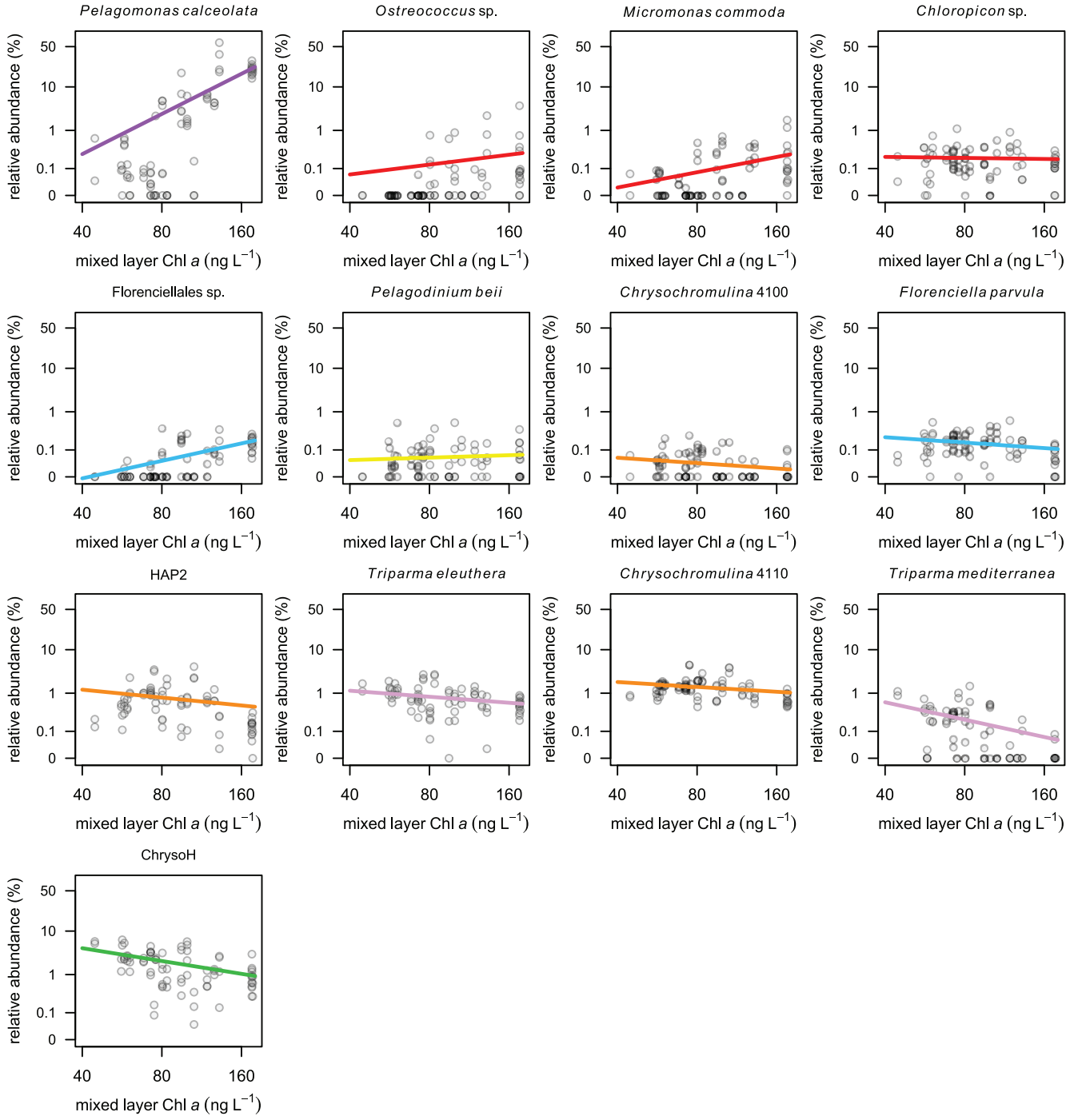

FIGURE 4 Niches of phytoplankton OTUs in response to variation in mixed layer Chl *a*. Relative abundance (proportion of reads) of samples within the mixed layer is plotted vs. mean Chl *a* concentration in the mixed layer, and the curves display the fitted logistic curves from a beta-binomial GLMM. The slope parameters of these curves are subsequently compared to the grazing ability of the corresponding isolate (Figure 5B). To facilitate visual comparison of OTU slopes, the y-axes are logit transformed and have the same limits on each panel. Panels are titled using the name of the corresponding isolate. The four top panels are autotrophs, and the subsequent mixotroph panels are sorted by grazing ability from left to right and top to bottom. Colours of the fitted curves correspond to the taxa colour scheme in Figure 2 (purple = pelagophyte, red = prasinophyte, blue = dictyochophyte, yellow = dinoflagellate, orange = haptophyte, purple = bolidophyte, green = chrysophyte).

dinoflagellate genus *Pelagodinium*, and chrysophyte clade H (Table S1). When correlating depth niches at Station ALOHA with grazing ability, mixotrophs tend to become more abundant near the surface while autotrophs tend to become more abundant at depth, with some overlap in response between these groups (Figure 2). There is an overall significant relationship between grazing ability and depth niche (χ^2_1 =6.3,

$p = 0.012$, $R^2 = 0.38$), and within the mixotrophs there is a tendency for faster-grazing taxa to have shallower niches ($\chi^2_1 = 3.1$, $p = 0.076$, $R^2 = 0.31$). The association between grazing ability and depth is moderately stronger when allowing depth niches to be nonlinear (all phytoplankton: $\chi^2_6 = 43$, $p < 10^{-6}$, $R^2 = 0.46$; mixotrophs: $\chi^2_6 = 23$, $p < 10^{-3}$, $R^2 = 0.40$; Figure S2).

Temporal correlates of trophic strategies in the mixed layer

The photic zone at Station ALOHA is permanently stratified, but mixed layer depth varies over time, with deeper mixing in the winter and spring (Karl et al., 2012; Figure S1). Previous analyses of the picoeukaryote community showed that mixing within the mixed layer has a homogenizing effect on community structure, and that seasonal cycles of community structure are more evident at shallower depths (Rii et al., 2022). The focal OTUs in this study respond differentially to mixed layer depth; for example relative abundances of *Pelagomonas* and Florenciellales_X increase steeply with MLD, while *Chrysochromulina* and *Triparma* tend to decline (Figure 3).

Previous analysis of phytoplankton trophic strategies found that increased stratification and reduced Chl *a* were associated with more phagotrophy (Edwards, Li, McBeain, et al., 2023). When analysing phytoplankton trophic strategies at Station ALOHA as a function of mixed layer depth, we found that mixotrophs tend to increase in relative abundance when the mixed layer is shallower, while autotrophs increase under deeper mixing (Figure 5A). There is a slightly stronger relationship when using mean MLD over the prior 14 days as a predictor ($\chi^2_1 = 6.4$, $p = 0.01$, $R^2 = 0.42$), compared to MLD during the sampling cruise ($\chi^2_1 = 3.7$, $p = 0.05$, $R^2 = 0.27$) or mean MLD over the prior 7 days ($\chi^2_1 = 4.8$, $p = 0.03$, $R^2 = 0.34$). Allowing for nonlinear MLD niches does not substantially strengthen the relationship with grazing ability ($\chi^2_4 = 21$, $p = 0.004$, $R^2 = 0.40$; Figure S3). Within the mixotrophs, there is a tendency for faster-grazing mixotrophs to respond more positively to shallower MLD, though the relationship is not statistically clear ($\chi^2_1 = 2.2$, $p = 0.14$, $R^2 = 0.25$).

Chl *a* concentrations at shallower depths exhibit fairly consistent seasonality at Station ALOHA, with peak values in Dec-Jan ~50% higher than the generally low values from April-Sept (Winn et al., 1995, White et al., 2015; Figure S1). If we define an OTU's 'Chl *a* niche' as the slope of relative abundance vs. Chl *a* (Figure 4), using only mixed layer samples, then there is a significant relationship between trophic strategy and Chl *a* niche (Figure 5B). Mixotrophs tend to become relatively more abundant than autotrophs as Chl *a* declines (grazing ability vs. Chl *a* niche: $\chi^2_1 = 8.3$,

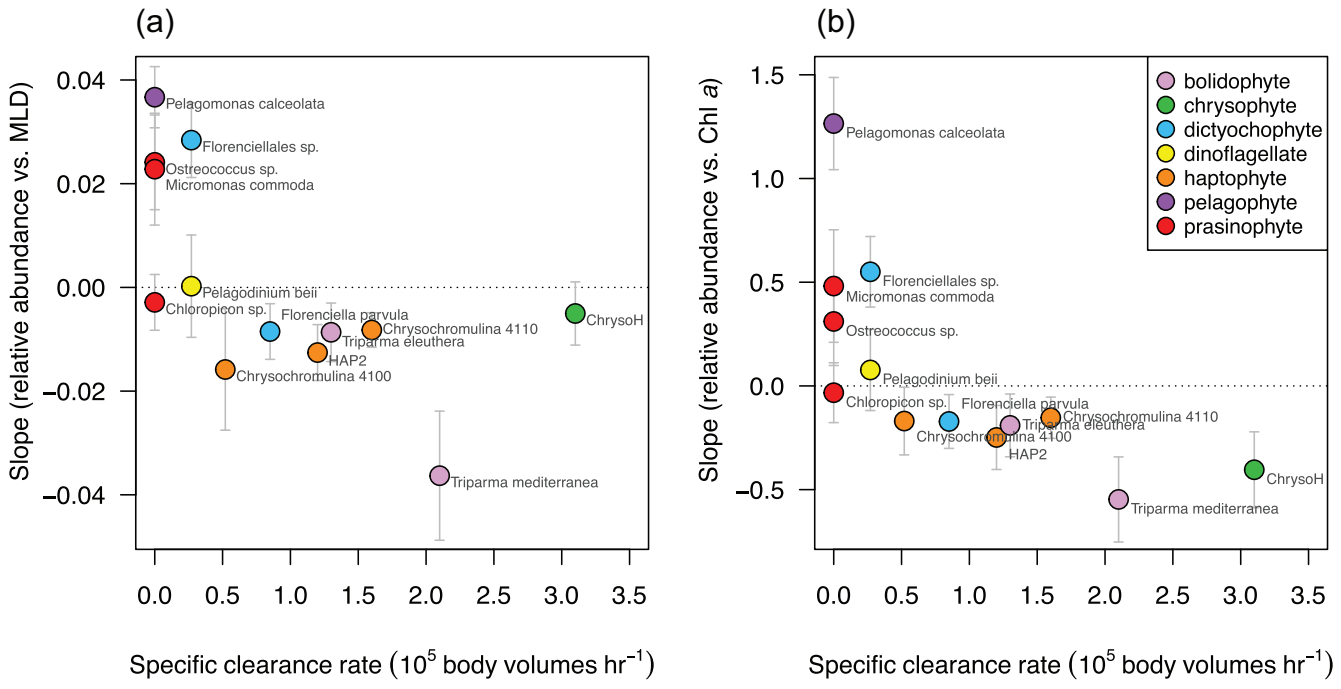

FIGURE 5 Grazing abilities of phytoplankton isolates compared to OTU niches, defined as the OTU response to temporal variation in mixed layer depth (A) and mixed layer Chl *a* (B). The y-axis is the slope of relative abundance vs. the environmental variable from a beta-binomial GLMM (Figures 3 and 4), with 95% CI error bars. The x-axis is grazing ability quantified as the body volume-specific clearance rate when consuming *Prochlorococcus*. Four autotrophic OTUs are given values of zero on the x-axis. Text adjacent to the points displays the names of the isolates.

$p = 0.004$, $R^2 = 0.52$), and there is a relationship within the mixotrophs as well, such that faster-grazing OTUs increase more steeply at low Chl *a* ($\chi^2_1 = 3.7$, $p = 0.054$, $R^2 = 0.40$). These relationships are moderately stronger when allowing Chl *a* niches to be nonlinear ($\chi^2_5 = 30$, $p < 10^{-4}$, $R^2 = 0.68$, and $\chi^2_5 = 15$, $p = 0.01$, $R^2 = 0.40$, respectively; Figure S4).

Seasonal and episodic dynamics across depths

To assess how seasonal and episodic dynamics of trophic strategies vary with depth, we calculated a community average trophic strategy, defined as the weighted mean clearance rate of the focal phytoplankton community, where the weights are the relative abundances of the genera containing the focal OTUs. Variation in mean strategy is driven primarily by *Pelagomonas*, *Chrysochromulina*, chrysophyte clade H, and *Ostreococcus*, as these are the most abundant genera in the focal community (Figure S5). The general seasonal pattern in mean clearance rate is a shift from more phototrophy during October–March to more phagotrophy during April–September (Figure 6). The amplitude of this variation is greatest at intermediate depths (45–100 m), with a ~ 60–100% change in the community mean. The shift in trophic strategy across depths is of greater magnitude than the shift across seasons, especially when comparing 5 and 25 m to depths below 100 m

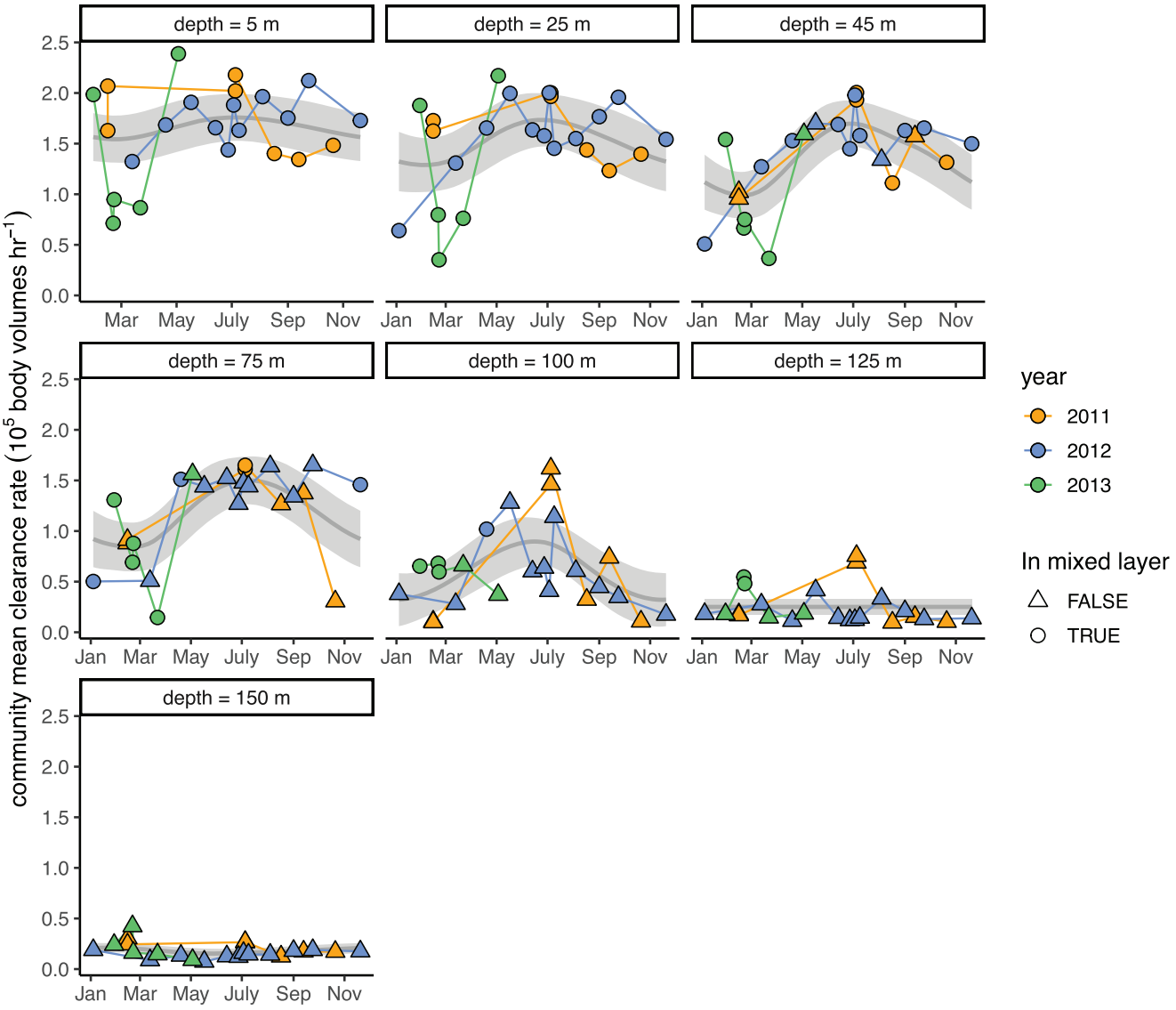

FIGURE 6 Temporal dynamics of community average grazing ability. The weighted mean specific clearance rate of the focal phytoplankton community (Figure S5) is plotted by day of year and depth, to visualize the community-wide shift in phytoplankton trophic strategy. Panel titles indicate the sample depth in meters. Grey curves and surrounding bands are fitted smoothers with 95% CI (generalized additive model with circular basis function). Circles and triangles indicate whether the sample was in the mixed layer or not, respectively.

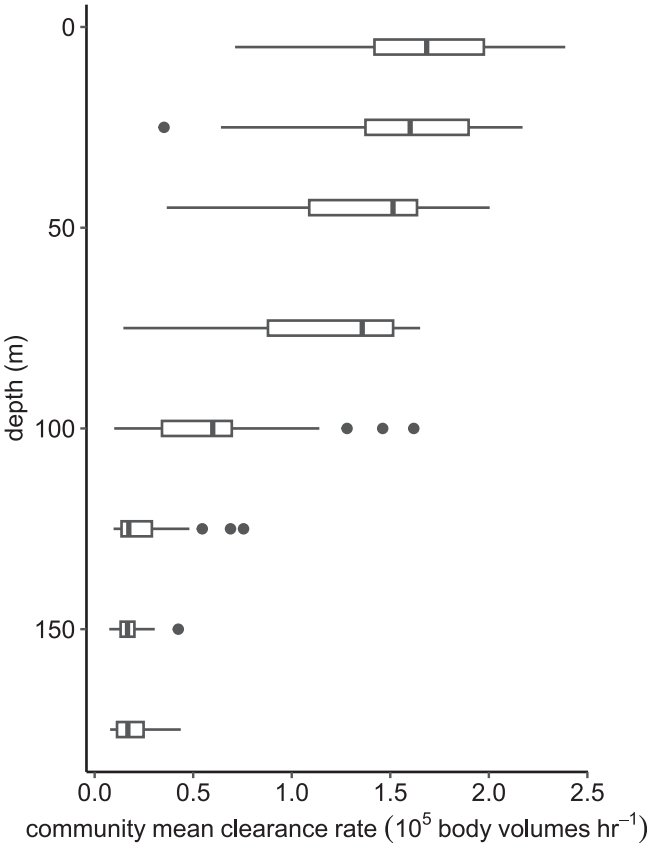

FIGURE 7 Community average grazing ability vs. depth. The weighted mean specific clearance rate of the focal phytoplankton community (Figure S5) is plotted by depth, to visualize the community-wide shift in phytoplankton trophic strategy. Boxes show the 25th, 50th, and 75th percentiles, whiskers extend to 1.5*interquartile range, and points show samples beyond the whiskers.

(Figure 7). Therefore, these patterns are consistent with the MLD and Chl *a* correlations described above, but this analysis provides more insight into the temporal dynamics and depth-dependence of these patterns.

When considering shorter-term dynamics, there are fluctuations in the community average strategy that are consistent with the forcing events described in Rii et al. (2022). During the deepest mixing event (March 2013), there is a > 2-fold shift towards phototrophy, and then a subsequent recovery (Figure 6). This shift happens throughout the top 75 meters, consistent with a deepening mixed layer and entrainment of deeper, more phototrophic taxa. The shift may also reflect competitive dynamics in response to lower mixed-layer irradiance and potential nutrient entrainment. In late June - early July 2012, there was an episode of isopycnal uplift that only affected the lower photic zone. During that period, there was a > 2-fold shift towards phototrophy at 100 meters, but not at shallower depths (Figure 6). This is consistent with the more autotrophic taxa that prevail below 100 m being displaced upwards. In general, month-scale variability in community mean strategy is greater at shallower depths, and this contributes to fairly uniform variances in the top 75 meters (Figure 7), even though regular seasonal trends are weak at 5 and 25 m (Figure 6).

DISCUSSION

A unique combination of lab experiments on diverse isolates and an extensive survey of community composition allowed us to document shifts in phytoplankton trophic strategies with depth and over time at a well-studied site in the oligotrophic North Pacific. The temporal and spatial dynamics of phytoplankton trophic strategies at Station ALOHA are consistent with spatial patterns in trophic strategies previously documented using *Tara* Oceans data (Edwards, Li, McBeain, et al., 2023). The concordance of results across datasets collected by different researchers, using comparable but distinct methods, suggests that the major patterns are robust, multiscale features of ocean phytoplankton communities. Both analyses found a shift from phototrophy to phagotrophy when moving from deep in the photic zone to shallower depths. It is noteworthy that the previous finding using *Tara* Oceans data only had surface and DCM samples (Edwards, Li, McBeain, et al., 2023)., while the data described here had better resolution of temporal and depth community patterns, but the general pattern is the same. When considering community structure within the mixed layer, mixotrophs tend to increase in relative abundance in time periods and locations of greater stratification, and when mixed layer Chl *a* is lower. There is also a shift within the mixotroph community towards more phagotrophic taxa as Chl *a* declines. It is noteworthy that in both analyses the correlation between niches and trophic strategies was greater when considering niches along a Chl *a* gradient, compared to niches based on metrics of stratification. This may indicate that Chl *a* is a more sensitive indicator of the environmental variables that drive variation in trophic strategy, and it also highlights the potential utility of Chl *a* as a predictor of phytoplankton trophic strategies for applications where extensive community sampling is impractical. The magnitude of the shift in trophic strategy over time at ALOHA (a ~ 1.6-2-fold change in community mean clearance rate at intermediate depths) is smaller than the shift across spatial locations in the global ocean (a ~ 4-fold change across more than 10-fold variation in Chl *a*; Edwards, Li, McBeain, et al., 2023), which is sensible considering the modest seasonality at this location (e.g., ~1.5-fold variation in mean mixed layer Chl *a*). Both of these analyses have focused on relatively oligotrophic regions of the ocean, and it will be important to perform similar analyses that extend into more eutrophic regions where larger phytoplankton comprise the bulk of the phytoplankton community.

The consistency in patterns across analyses applies not only to the general correlation between niches and grazing ability but also to the niches of particular taxa. For example, the chrysophyte clade H OTU has one of the shallowest distributions, and one of the steepest increases as Chl *a* declines, in both analyses. The corresponding isolates have a particularly high specific clearance rate when consuming *Prochlorococcus*, and are obligate mixotrophs, requiring both light and prey to grow (Edwards, Li, McBeain, et al., 2023; Li et al., 2022). Therefore, this taxon may be particularly well adapted to living at shallow depths in permanently stratified waters, where dissolved nutrients are consistently scarce, concentrations of bacterial prey are fairly constant, and light is reliably plentiful. A Florenciellales OTU is the mixotroph that is most similar to the autotrophs in both analyses, with a fairly deep distribution and a positive response to increasing Chl *a*. The isolates corresponding to this OTU have a very low specific clearance rate, and this rate is lower than that of the *Florenciella parvula* isolates whose corresponding OTU has a shallower niche and a negative response to increasing Chl *a*. Among the autotrophic phytoplankton, in both analyses *Pelagomonas* and *Ostreococcus* OTUs tend to have the deepest niches and exhibit the greatest increases in relative abundance as Chl *a* increases, when compared to *Chloropicon* and *Micromonas*. Niche variation among autotrophs cannot be explained by the spectrum of trophic strategies that is the focus of this study, and therefore represents another dimension of phytoplankton trait variation, potentially driven by investments in photosynthesis vs. nutrient acquisition. In general, temporal dynamics and depth differentiation in protist composition similar to that found in Rii et al. (2022) have been observed in other oligotrophic regions, such as the eastern South Pacific (Shi et al., 2011), the eastern North Pacific (Choi et al., 2020), and the subtropical North Atlantic (Blanco-Bercial et al., 2022), suggesting that protist community structure may be relatively predictable across depths and at seasonal timescales. In addition, the temporal dynamics in community function described here, with a focus on the smallest eukaryotic phytoplankton, are consistent with dynamics observed among the largest eukaryotic phytoplankton in more productive waters. For example, in the North Atlantic, autotrophic diatoms dominate in the winter and spring, while plastid-bearing dinoflagellates (presumed to be mixotrophic) increase in relative abundance during the summer and fall, briefly overtaking diatoms during August (Barton et al., 2013). However, whether there are also seasonal shifts in trophic strategy within the mixotrophic microphytoplankton remains to be studied.

Disentangling the mechanisms underlying the temporal dynamics of trophic strategies is challenging, because irradiance, dissolved nutrients, temperature, and other factors tend to covary over time and with depth. Models show that lower nutrient supply benefits relatively phagotrophic phytoplankton, in competition with autotrophs and relatively phototrophic mixotrophs (Edwards, Li, McBeain, et al., 2023; Ward et al., 2011), while higher irradiance benefits mixotrophs in competition with heterotrophs (Edwards, Li, McBeain, et al., 2023; Rothhaupt, 1996). The result is that conditions of scarce nutrients and high irradiance are most beneficial for mixotrophs, and relatively phagotrophic mixotrophs in particular. These conclusions are consistent with other models investigating seasonal variation in trophic strategy, which find that stratified 'summer' conditions favour mixotrophs (Chakraborty et al., 2017; Leles et al., 2021). The temporal dynamics and depth differentiation observed at Station ALOHA are consistent with the hypothesized dual role of light and nutrient limitation in driving trophic strategies. A deeper mixed layer, which reduces the integrated irradiance available to phytoplankton, and which may be associated with nutrient entrainment and greater turbulent diffusion across the nutricline, is associated with a shift towards phototrophy. Similarly, the greater nutrient concentrations and lower irradiance at depth are associated with a shift to phototrophy. Deepening of the mixed layer should entrain relatively phototrophic taxa from below the mixed layer, and therefore the association between mixed layer depth and trophic strategy is likely a combination of short-term entrainment and longer-term competition between trophic strategies. It is interesting that the community mean trophic strategy shows the greatest temporal fluctuation at intermediate depths. This is consistent with the importance of shifts in light and nutrient limitation, because photosynthesis is light-saturated at depths ≤45 m throughout the year (Li et al., 2011), and the bottom of the photic zone is light-limited, while intermediate depths likely shift in the degree of light and nutrient limitation as downwelling irradiance shifts seasonally, and as these depths enter and exit the mixed layer. Diversity of the total picoeukaryote community peaks at 75 m (Rii et al., 2022), which could be driven in part by the co-occurrence of diverse trophic strategies that shift in relative importance over time.

Gradients of prey availability may reinforce shifts in trophic strategy driven by light and nutrient availability, because the concentrations of both *Prochlorococcus* and heterotrophic bacteria tend to be greatest in the upper ~75 m at this site (Figure S6), and steadily decline below that. This further increases the ratio of nutrients in prey biomass to dissolved nutrients at shallower depths, which should select for phagotrophy (Edwards, Li, McBeain, et al., 2023). Temperature variation could also reinforce shifts in trophic strategy, as higher temperatures are associated with more light and less dissolved nutrients, and heterotrophic metabolism tends to increase faster than autotrophic metabolism with rising temperatures (Wilken

et al., 2013), which could increase the payoff of investing in phagotrophy at higher temperatures. The strong correlation of trophic strategies with mixed layer Chl *a* may occur because Chl *a* is a function of biomass, which tends to increase with nutrient supply, and also a function of photoacclimation, which responds to irradiance (more irradiance = less Chl *a*) as well as nutrient supply (less nutrients = less Chl *a*). At Station ALOHA, variation in mixed layer Chl *a* is thought to be primarily driven by photoacclimation (Winn et al., 1995, Letelier et al., 2017). In addition, change in community composition may itself contribute to variation in Chl *a*, if relatively phagotrophic mixotrophs contain less Chl *a* per C, and/or if a shift towards phagotrophy increases consumption of smaller photoautotrophs.

The patterns of trophic strategy we have documented could have various ecosystem consequences that might be explored in future research. For example, the proportion of carbon fixation that is supported by nutrients from ingested prey may vary systematically with depth and season, although it is unclear how large that fraction can become. Similarly, the rate of bacterial ingestion and the efficiency with which that biomass is transferred up the food chain may also vary systematically, if the abundance of mixotrophs relative to heterotrophs exhibits patterns similar to those found when comparing mixotrophs to autotrophs. In general, our understanding of microbial food web processes would be aided by a greater understanding of which heterotrophic protists compete with mixotrophs for *Prochlorococcus* and other bacterial taxa, and how their ecophysiologies compare to the spectrum of mixotroph strategies.

AUTHOR CONTRIBUTIONS

Kyle F. Edwards: Conceptualization; methodology; funding acquisition; visualization; writing – original draft; writing – review and editing; investigation; formal analysis. **Yoshimi M. Rii:** Conceptualization; methodology; writing – review and editing; investigation; formal analysis. **Qian Li:** Investigation; conceptualization; methodology; writing – review and editing; formal analysis. **Logan M. Peoples:** Conceptualization; methodology; investigation; writing – review and editing; formal analysis. **Matthew J. Church:** Conceptualization; methodology; investigation; funding acquisition; writing – review and editing. **Grieg F. Steward:** Conceptualization; methodology; investigation; funding acquisition; writing – review and editing.

ACKNOWLEDGEMENTS

This work was supported by NSF grant 2224832 to KFE and GFS. MJC acknowledges the Simons Foundation for support of the SCOPE program (award 721221). We thank the HOT program science team for their assistance and for providing contextual data used in this study. This publication includes observations from the WHOI-Hawaii Ocean Time series Site (WHOTS) mooring, which is supported by the National Oceanic and Atmospheric Administration (NOAA) through the Cooperative Institute for Climate and Ocean Research (CICOR) under grants NA17RJ1223 and NA090AR4320129 to the Woods Hole Oceanographic Institution, and by the National Science Foundation grants to the HOT program.

CONFLICT OF INTEREST STATEMENT

The author declares no conflict of interest.

DATA AVAILABILITY STATEMENT

The data that support the findings of this study are openly available in figshare at https://doi.org/10.6084/m9.figshare.25587411.

ORCID

Kyle F. Edwards https://orcid.org/0000-0002-0661-3903
Yoshimi M. Rii https://orcid.org/0000-0002-6486-8955
Qian Li https://orcid.org/0000-0001-9977-7482
Logan M. Peoples https://orcid.org/0000-0002-0163-2769
Matthew J. Church https://orcid.org/0000-0002-6166-8579
Grieg F. Steward https://orcid.org/0000-0001-5988-0522

REFERENCES

Barton, A.D., Finkel, Z.V., Ward, B.A., Johns, D.G. & Follows, M.J. (2013) On the roles of cell size and trophic strategy in North Atlantic diatom and dinoflagellate communities. *Limnology and Oceanography*, 58, 254–266. Available from: https://doi.org/10.4319/lo.2013.58.1.0254

Blanco-Bercial, L., Parsons, R., Bolaños, L.M., Johnson, R., Giovannoni, S.J. & Curry, R. (2022) The protist community traces seasonality and mesoscale hydrographic features in the oligotrophic Sargasso Sea. *Frontiers in Marine Science*, 9, 897140.

Brooks, M.E., Kristensen, K., Van Benthem, K.J., Magnusson, A., Berg, C.W., Nielsen, A. et al. (2017) glmmTMB balances speed and flexibility among packages for zero-inflated generalized linear mixed modeling. *The R Journal*, 9, 378–400.

Chakraborty, S., Nielsen, L.T. & Andersen, K.H. (2017) Trophic strategies of unicellular plankton. *The American Naturalist*, 189, E77–E90. Available from: https://doi.org/10.1086/690764

Choi, C.J., Jimenez, V., Needham, D.M., Poirier, C., Bachy, C., Alexander, H. et al. (2020) Seasonal and geographical transitions in eukaryotic phytoplankton community structure in the Atlantic and Pacific oceans. *Frontiers in Microbiology*, 11, 542372.

de Boyer Montégut, C., Madec, G., Fischer, A.S., Lazar, A. & Iudicone, D. (2004) Mixed layer depth over the global ocean: an examination of profile data and a profile-based climatology. *Journal of Geophysical Research, Oceans*, 109, C12.

De Vargas, C., Audic, S., Henry, N., Decelle, J., Mahé, F., Logares, R., Lara, E., Berney, C., Le Bescot, N., Probert, I. & Carmichael, M. (2015) Eukaryotic plankton diversity in the sunlit ocean. *Science*, 348(6237), 1261605.

Edwards, K.F. (2019) Mixotrophy in nanoflagellates across environmental gradients in the ocean. *Proceedings. National Academy of Sciences. United States of America*, 116, 6211–6220. Available from: https://doi.org/10.1073/pnas.1814860116

Edwards, K.F., Li, Q., McBeain, K.A., Schvarcz, C.R. & Steward, G.F. (2023) Trophic strategies explain the ocean niches of small eukaryotic phytoplankton. *Proceedings of the Royal Society B*, 290, 20222021. Available from: https://doi.org/10.1098/rspb.2022.2021

Edwards, K.F., Li, Q. & Steward, G.F. (2023) Ingestion kinetics of mixotrophic and heterotrophic flagellates. *Limnology and Oceanography*, 68, 917–927. Available from: https://doi.org/10.1002/lno.12320

Frias-Lopez, J., Thompson, A., Waldbauer, J. & Chisholm, S.W. (2009) Use of stable isotope-labelled cells to identify active grazers of picocyanobacteria in ocean surface waters. *Environmental Microbiology*, 11, 512–525. Available from: https://doi.org/10.1111/j.1462-2920.2008.01793.x

Guillou, L., Bachar, D., Audic, S., Bass, D., Berney, C., Bittner, L. et al. (2012) The Protist ribosomal reference database (PR2): a catalog of unicellular eukaryote small sub-unit rRNA sequences with curated taxonomy. *Nucleic Acids Research*, 41, D597–D604.

Karl, D.M., Church, M.J., Dore, J.E., Letelier, R.M. & Mahaffey, C. (2012) Predictable and efficient carbon sequestration in the North Pacific Ocean supported by symbiotic nitrogen fixation. *Proceedings. National Academy of Sciences. United States of America*, 109, 1842–1849. Available from: https://doi.org/10.1073/pnas.1120312109

Leles, S.G., Bruggeman, J., Polimene, L., Blackford, J., Flynn, K.J. & Mitra, A. (2021) Differences in physiology explain succession of mixoplankton functional types and affect carbon fluxes in temperate seas. *Progress in Oceanography*, 190, 102481.

Letelier, R.M., White, A.E., Bidigare, R.R., Barone, B., Church, M.J. & Karl, D.M. (2017) Light absorption by phytoplankton in the North Pacific Subtropical Gyre. *Limnology and Oceanography*, 62(4), 1526–1540.

Li, B., Karl, D.M., Letelier, R.M. & Church, M.J. (2011) Size-dependent photosynthetic variability in the North Pacific subtropical gyre. *Marine Ecology Progress Series*, 440, 27–40.

Li, Q., Edwards, K.F., Schvarcz, C.R. & Steward, G.F. (2022) Broad phylogenetic and functional diversity among mixotrophic consumers of Prochlorococcus. *The ISME Journal*, 16, 1557–1569.

Mitra, A., Caron, D.A., Faure, E., Flynn, K.J., Leles, S.G., Hansen, P.J. et al. (2023) The Mixoplankton database (MDB): diversity of photo-phago-trophic plankton in form, function, and distribution across the global ocean. *Journal of Eukaryotic Microbiology*, 70, e12972. Available from: https://doi.org/10.1111/jeu.12972

Mitra, A., Flynn, K.J., Burkholder, J.M., Berge, T., Calbet, A., Raven, J.A. et al. (2014) The role of mixotrophic protists in the biological carbon pump. *Biogeosciences*, 11, 995–1005.

Partensky, F., Hess, W.R. & Vaulot, D. (1999) *Prochlorococcus*, a marine photosynthetic prokaryote of global significance. *Microbiology and Molecular Biology Reviews*, 63, 106–127. Available from: https://doi.org/10.1128/MMBR.63.1.106-127.1999

Pasulka, A.L., Landry, M.R., Taniguchi, D.A., Taylor, A.G. & Church, M.J. (2013) Temporal dynamics of phytoplankton and heterotrophic protists at station ALOHA. *Deep Sea Research Part II: Topical Studies in Oceanography*, 93, 44–57.

Pierella Karlusich, J.J., Ibarbalz, F.M. & Bowler, C. (2020) Phytoplankton in the *Tara* Ocean. *Annual Review of Marine Science*, 12, 233–265. Available from: https://doi.org/10.1146/annurev-marine-010419-010706

Rii, Y.M., Duhamel, S., Bidigare, R.R., Karl, D.M., Repeta, D.J. & Church, M.J. (2016) Diversity and productivity of photosynthetic picoeukaryotes in biogeochemically distinct regions of the south East Pacific Ocean. *Limnology and Oceanography*, 61, 806–824. Available from: https://doi.org/10.1002/lno.10255

Rii, Y.M., Peoples, L.M., Karl, D.M. & Church, M.J. (2022) Seasonality and episodic variation in picoeukaryote diversity and structure reveal community resilience to disturbances in the North Pacific subtropical gyre. *Limnology and Oceanography*, 67, S331–S351. Available from: https://doi.org/10.1002/lno.11916

Rothhaupt, K.O. (1996) Laboratorary experiments with a Mixotrophic Chrysophyte and Obligately Phagotrophic and photographic competitors. *Ecology*, 77, 716–724. Available from: https://doi.org/10.2307/2265496

Shi, X.L., Lepère, C., Scanlan, D.J. & Vaulot, D. (2011) Plastid 16S rRNA gene diversity among eukaryotic picophytoplankton sorted by flow cytometry from the South Pacific Ocean. *PloS One*, 6(4), e18979.

Ward, B.A., Dutkiewicz, S., Barton, A.D. & Follows, M.J. (2011) Biophysical aspects of resource acquisition and competition in algal Mixotrophs. *The American Naturalist*, 178, 98–112. Available from: https://doi.org/10.1086/660284

Ward, B.A. & Follows, M.J. (2016) Marine mixotrophy increases trophic transfer efficiency, mean organism size, and vertical carbon flux. *Proceedings. National Academy of Sciences. United States of America*, 113, 2958–2963. Available from: https://doi.org/10.1073/pnas.1517118113

White, A.E., Letelier, R.M., Whitmire, A.L., Barone, B., Bidigare, R.R., Church, M.J. et al. (2015) Phenology of particle size distributions and primary productivity in the North Pacific subtropical gyre (Station ALOHA). *JGR Oceans*, 120, 7381–7399. Available from: https://doi.org/10.1002/2015JC010897

Wilken, S., Huisman, J., Naus-Wiezer, S. & Van Donk, E. (2013) Mixotrophic organisms become more heterotrophic with rising temperature. *Ecology Letters*, 16, 225–233.

Wilken, S., Yung, C.C.M., Poirier, C., Massana, R., Jimenez, V. & Worden, A.Z. (2023) Choanoflagellates alongside diverse uncultured predatory protists consume the abundant open-ocean cyanobacterium *Prochlorococcus*. *Proceedings. National Academy of Sciences. United States of America*, 120, e2302388120. Available from: https://doi.org/10.1073/pnas.2302388120

Winn, C.D., Campbell, L., Christian, J.R., Letelier, R.M., Hebel, D.V., Dore, J.E. et al. (1995) Seasonal variability in the phytoplankton community of the North Pacific subtropical gyre, global Biogeochem. *Cycle*, 9, 605–620. Available from: https://doi.org/10.1029/95GB02149

Yeh, Y.-C. & Fuhrman, J.A. (2022) Contrasting diversity patterns of prokaryotes and protists over time and depth at the san-Pedro Ocean time series. *ISME Communications*, 2, 36.

SUPPORTING INFORMATION

Additional supporting information can be found online in the Supporting Information section at the end of this article.

How to cite this article: Edwards, K.F., Rii, Y.M., Li, Q., Peoples, L.M., Church, M.J. & Steward, G.F. (2024) Trophic strategies of picoeukaryotic phytoplankton vary over time and with depth in the North Pacific Subtropical Gyre. *Environmental Microbiology*, 26(8), e16689. Available from: https://doi.org/10.1111/1462-2920.16689